Hindawi Publishing Corporation
Journal of Nanomaterials
Volume 2015, Article ID 546851, 7 pages
http://dx.doi.org/10.1155/2015/546851

Research Article

Configuration Transitions of Free Circular DNA System Induced by Nicks

Chao Ji,[1,2] Lingyun Zhang,[1] and Pengye Wang[1]

[1]*Beijing National Laboratory for Condensed Matter Physics, Institute of Physics, Chinese Academy of Sciences, Beijing 100190, China*
[2]*College of Biological Science, Weifang Medical University, Shandong 261053, China*

Correspondence should be addressed to Lingyun Zhang; lyzhang@iphy.ac.cn and Pengye Wang; pywang@iphy.ac.cn

Received 27 May 2015; Accepted 7 July 2015

Academic Editor: Song Cui

Nicks have important functions in the biological functions of DNA-mediated systems. However, the configuration transitions of DNA molecules induced by the presence of nicks have not been quantitatively investigated. This study aims to analyze the configuration transitions of free circular DNA system induced by nicks. Using atomic force microscopy, two configuration states were observed in the free circular DNA system with different nick numbers. To understand the transmission of torsional energy among DNA base pairs, we defined the effective length and nicking angle. In the free DNA system, a torsional energy of 233 bp can be completely released by nicks. Based on the experimental and quantitative results, we propose a physical mechanism to explain the configuration transitions of the free circular DNA system induced by nicks. This study and the presented method are very useful in understanding the physical mechanism of nicks in DNA-mediated systems.

1. Introduction

A nick is a discontinuity in the double helical structure of DNA. It is a single-strand break in which a phosphodiester bond between adjacent nucleotides is cleaved [1]. Nicked DNA has an important function in the biological functions of cell processes. Topoisomerase I of the DNA recombination system creates transient DNA break via a covalent bond between the cleaved strand and the enzyme; this break is generally initiated by nicks on base pairs (bp) [2, 3]. Nicked DNA has also been used in the study of the base excision repair pathway, which is the primary repair system used to maintain the genome integrity in mammalian cells [4–7]. In addition, double nicking is applied to enhance genome editing specificity in targeted genome editing technologies [8–10]. And the crystal structures of polymerase β complex with nicked DNA reveal that polymerase β binds nicked DNA with a 90° kink [11]. This finding demonstrates that nicked DNA is more flexible than double-stranded DNA. Thus, nicked DNA is more prone to changes in configuration. Proteins can be stimulated by nicks to bind to DNA and carry out their specific biological functions [12]. However, configuration transitions of DNA molecules induced by the presence of nicks have yet to be quantitatively investigated. Its investigation will be very helpful in understanding the important function of the DNA configuration transitions. In this study, we present a method to analyze quantitatively the configuration transitions of circular DNA induced by nicks using atomic force microscopy (AFM). We studied the configuration states of circular DNA containing different numbers of nicks. We observed two (flat circular and intersecting states) configuration states in the circular DNA system. Further, for revealing the physical property of nicks in DNA molecules, we defined the effective length, release length, and nicking angle in topological analysis to study the transmission of torsional energy. In the free DNA system, a torsional energy of 233 bp can be released by nicks.

Based on experimental and quantitative results, we propose a mechanism to explain the configuration transitions of the free circular DNA under the influence of nicks. Nicks can release the torsional energy of local bp in DNA molecules. The present findings are valuable in understanding the behavior of nicks in free DNA system.

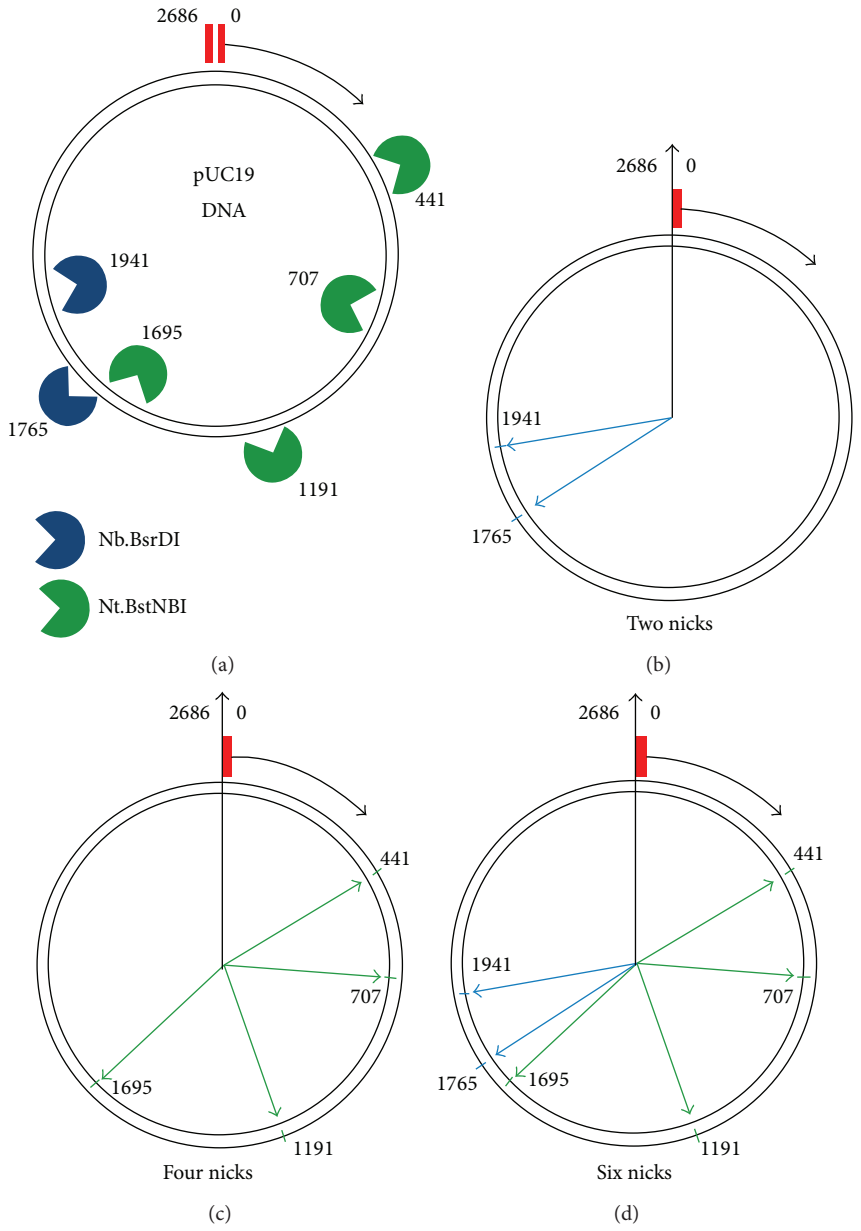

Figure 1: Nicking sites in pUC19 DNA were produced by two nicking endonucleases (a). The blue and green symbols represent Nb.BsrDI and Nt.BstNBI, respectively. Schematic of angle degrees on pUC19 DNA produced by two nicking endonucleases (b–d). Nicking angles of pUC19 DNA with (b) two, (c) four, and (d) six nicks.

2. Materials and Methods

2.1. Materials. In the experiments, pUC19, a commonly used plasmid and cloning vector for *Escherichia coli*, was purchased from New England Biolabs. The molecule is a double-stranded circular plasmid having a length of 2,686 bp. Two nicking endonucleases, each cleaving only one strand of a double-stranded DNA substrate, were also purchased from New England Biolabs.

2.2. Chemical Reagents. In the experiments, Nb.BsrDI and Nt.BstNBI, two nicking endonucleases, were used to produce nicked pUC19 [13–15]. The recognition sites of two nicking endonucleases on pUC19 DNA are shown in Figure 1(a). According to induction of New England Biolabs, a total reaction volume of 50 μL containing 2 μg of closed circular pUC19 DNA and ten units of Nb.BsrDI in NEB buffer 2 were incubated for 3 h at 65°C. The mixture was incubated for 20 min at 80°C to quench the reaction, and the nicked pUC19 was purified from this reaction mixture by a centrifugal filter (Millipore Microcon). The reaction buffer (20 μL) containing ten units of Nt.BstNBI and closed circular pUC19 DNA (2 μg) was incubated at 55°C for 3 h. The reaction was then heated to 80°C for 20 min and purified using the same method as

described above. Nicked pUC19 DNA was also digested by Nt.BstNBI according to the method described above. Nicked circular pUC19 DNA with a varying number of nicks was obtained with the aid of two nicking endonucleases.

2.3. Preparation of Samples. AFM experiments were carried out to study the configuration transitions of plasmid DNA. All samples were performed in a solution of 10 mM Tris-HCl, pH 7.5, and the concentration of DNA used was 0.12 ng/μL [16]. For AFM imaging, a reaction volume of 20 μL containing 5 mM $MgCl_2$ was used. The mixture was deposited on the surface of freshly cleaved mica. After 15 min, the mica surface was washed several times with 200 μL of Milli-Q filtered ultrapure water and then blown dry by a gentle stream of nitrogen gas [17].

2.4. AFM. In this study, all images were obtained under ambient conditions using a multimode AFM with a Nanoscope IIIa controller (Digital Instruments, Santa Barbara, CA, USA) in tapping mode. A silicon RTESP14 probe from Veeco (USA) was used at a resonance frequency range of 314 kHz to 316 kHz. The "E" scanner was used in the experiments. The scan frequency was 1 Hz per line, and the scan size ranged from 1 μm to 4 μm. All AFM images at a resolution of 512 × 512 pixels were not modified, except to flatten them.

3. Results and Discussion

Using AFM, we observed the configuration transitions of pUC19 DNA in the presence of nicks. Full, three-dimensional views with equilibrium conformations of DNA in solution are difficult to obtain. However, under appropriate experimental conditions, DNA can adhere to a mica surface weakly enough so that the interaction between DNA and mica modified by Mg^{2+} does not affect the equilibrium conformations of DNA in two-dimensional views, unlike the interaction between DNA and mica modified by 3-aminopropyltriethoxysilane [18]. As shown in Figure 2(a), pUC19 DNA can be distinguished based on morphological differences. pUC19 molecules are circular and rarely intersect. A quantitative geometric analysis for every DNA molecule was performed to study the configuration states in detail. In the AFM images, the configuration states of the pUC19 DNA can be classified into two types (flat circular and intersecting forms) according to the geometric shape of a single circular DNA molecule. The flat circular form (Figure 2(b)) does not intersect or twist within itself. The intersecting form is demonstrated in Figure 2(c).

Using two nicking endonucleases, we studied the configuration transitions of the pUC19 DNA containing nicks. Figure 3 demonstrates configuration transitions of pUC19 DNA induced by a varying number of nicks. In Figure 3(a), there are a lot of circular DNA molecules with intersection form. Then, the quantity of intersection form decreases as shown in Figure 3(b), which reveals the configuration transition from intersection form to flat circular form under the influence of two nicks. When four nicks exist in the

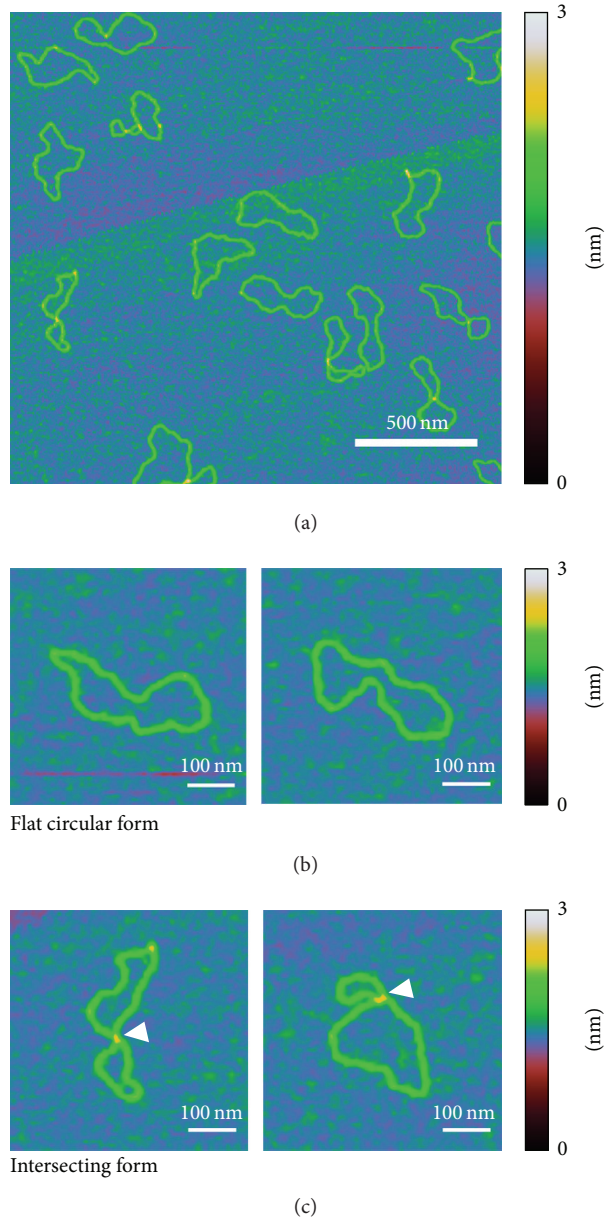

Figure 2: AFM images of natural pUC19 DNA in the absence of nicks (a). Representative images of natural circular DNA with two configuration forms. Images of the (b) flat circular form and (c) intersecting form.

circular DNA, there are many DNA configurations with flat circular form and little intersection form as indicated by Figure 3(c). This result indicates that the occurrence of intersection form is obviously decreased as the increase of nick numbers. In comparison with six nicks shown in Figure 3(d), it is not obviously different from Figure 3(c) on the configuration forms. Further, circular DNA molecules were measured in the closed form or with two, four, or six nicks to analyze quantitatively the configuration of every circular DNA molecule on the mica surface. As described above, the free circular DNA system has two configuration

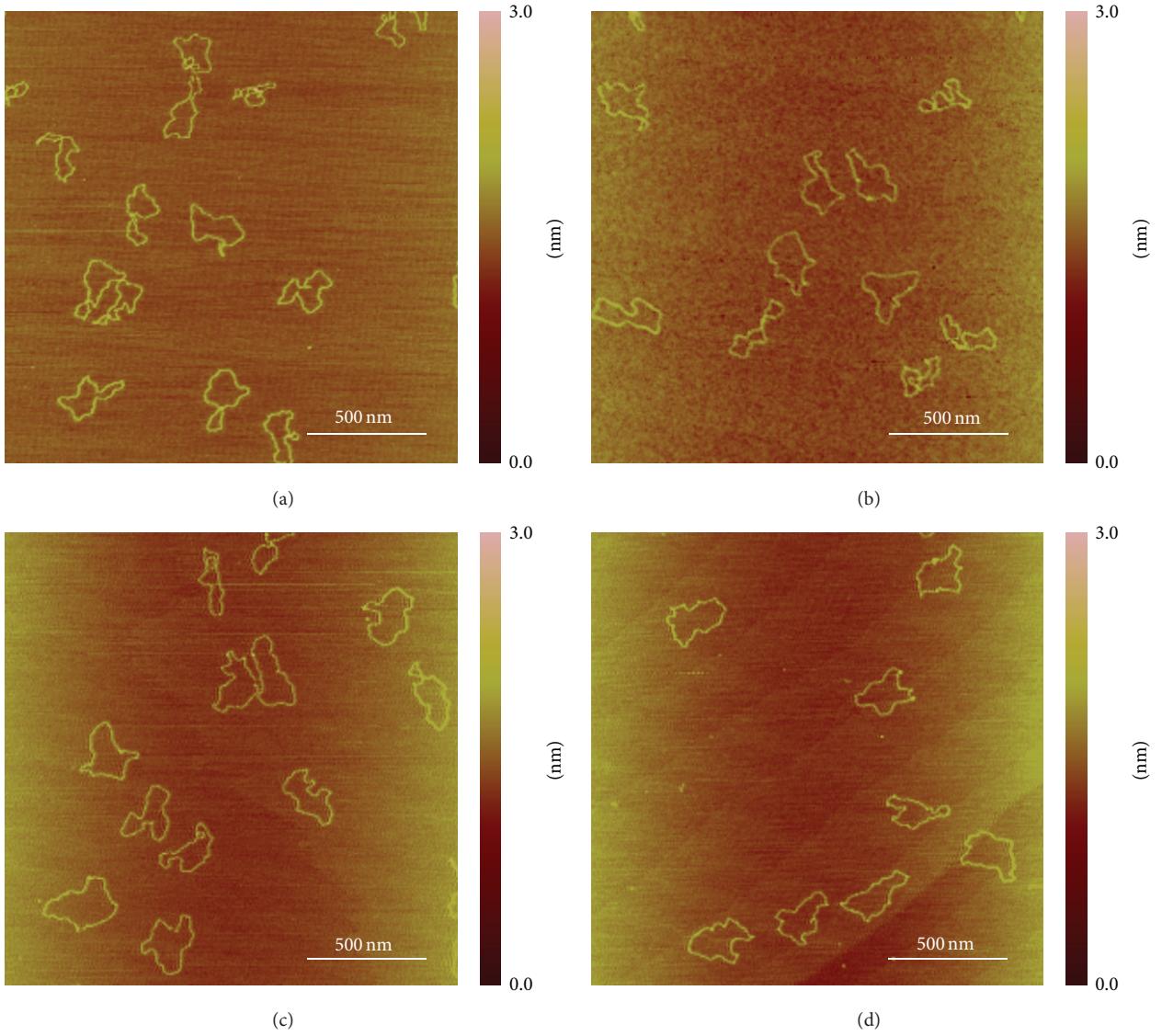

Figure 3: Representative images of circular DNA with different numbers of nicks. (a) Without nick; (b) with two nicks; (c) with four nicks; (d) with six nicks.

states (Figure 4 and Table SI in Supplementary Materials available online at http://dx.doi.org/10.1155/2015/546851). As shown in Figure 4, 75% and 25% of the closed DNA take the flat circular and intersecting forms, respectively. In circular DNA with two nicks, the occurrence of the flat circular and intersecting forms is increased to 82% and is decreased to 18%, respectively. For pUC19 DNA with four or six nicks, approximately 90% and 9% of the DNA take the flat circular and intersecting forms, respectively.

The nicking positions recognized by the two nicking endonucleases are shown in Figure 1(a), wherein the nicking angle shows the degree between the nicking sites and initial site of circular DNA on topological maps. The nicking angles of the pUC19 DNA are illustrated in Figures 1(b)–1(d) based on the topological map. The nicking angles of the two nicks in Figure 1(b) are 237° and 260°, and the nicking angles of the four nicks in Figure 1(c) are 59°, 95°, 160°, and 227°. The nicking angles of six nicks are produced by two nicking endonucleases (Figure 1(d)). The angle between two nicks is 23°, which is less than 7% of all circular DNA molecules. Thus, the intersecting state of circular DNA occurs in more than 18% of the molecules, and two nicks cannot completely release the torsional energy of a DNA molecule. The angles among four nicks are 168°, which includes three angles of 36°, 65°, and 67°. Compared with the angle of four nicks, the angle among six nicks is only increased to 33°, which is less than 10% of all circular DNA molecules. Thus, the pUC19 DNA with four and six nicks exhibits similar degrees of configuration states. Moreover, the nicking angles mainly occur between 59° and 260°. Thus, other angles of 160° are not affected by nicks. The nicking asymmetry leads to the torsional energy of circular DNA not being completely released. In addition, the occurrence of the intersecting state is approximately 9% in the presence of six nicks.

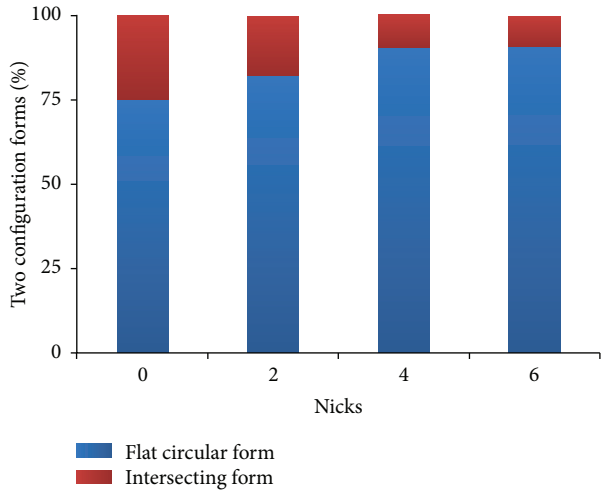

Figure 4: Quantitative results of pUC19 DNA with different numbers of nicks. Percentages of occurrences of the two forms of nicked pUC19 DNA without nicks (0), with two nicks (2), with four nicks (4), and with six nicks (6).

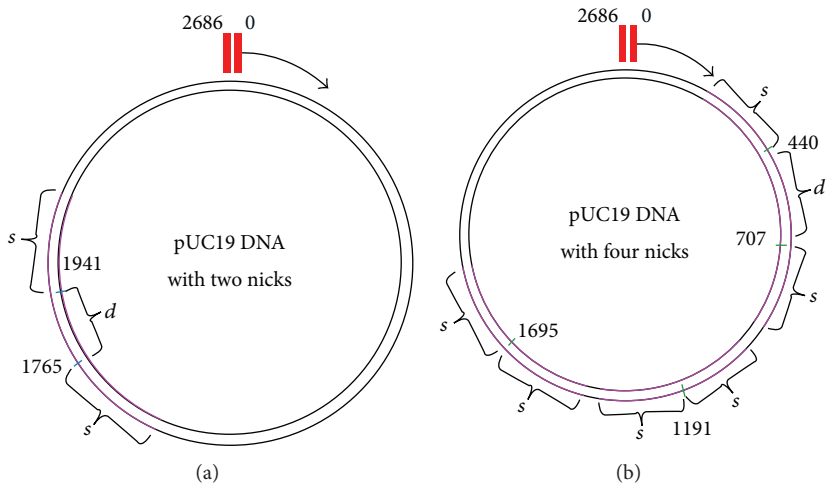

Figure 5: Schematic of the release length on pUC19 DNA produced by nicks. Pink segments indicate that torsional energy is completely released. Segments indicated by "*s*" represent the release length of base pairs induced by nicks. Segments indicated by "*d*" represent the distant length between two neighbor nicks, which should be less than the double release length by nicks. The rest of pUC19 DNA represented by the black segments is the effective length. Diagram of pUC19 DNA with (a) two and (b) four nicks.

According to the topological analysis of nicking angle and quantitative results of configuration states, we believe that local segments of circular DNA still store torsional energy. We define effective length as the storage capacity of bp for torsional energy and release length as the energy release of bp by a nick. In the two nicks shown in Figure 5(a), the full length of the pUC19 DNA is the sum of the double release length ("*s*"), the length between two nicks ("*d*"), and the effective length (black segments of the circular DNA). In the four nicks shown in Figure 5(b), the full length of the pUC19 DNA is the sum of the sixfold release length ("*s*"), length between 441 and 707 bp ("*d*"), and effective length (black segments of the pUC19 DNA). In the definitions, the effective length represents the storage capacity of torsional energy in the base pairs. The torsional energy of circular DNA molecules leads to the formation of an intersecting shape. We assumed that the amount of intersecting shapes can reflect the value of effective length. According to the quantitative results of configuration, the occurrence of the intersecting state with two nicks (18%) is approximately twice that with four nicks (10%). Thus, we can assume that the effective length of two nicks is also twice that of four nicks. Finally, we can calculate that the release length is 233 bp, suggesting that the torsional energy of 233 bp is completely released by a nick and also demonstrates the base pairs in transmission length of torsional energy in the free DNA system (the calculation is described in the Supplementary Materials). In order to study the physical property of nicked DNA molecules, the effect of tension on clustered nicks in DNA molecules is studied by applying tension on DNA molecules with optical tweezers [19]. However, this research cannot discuss the configuration transitions and torsional character under the

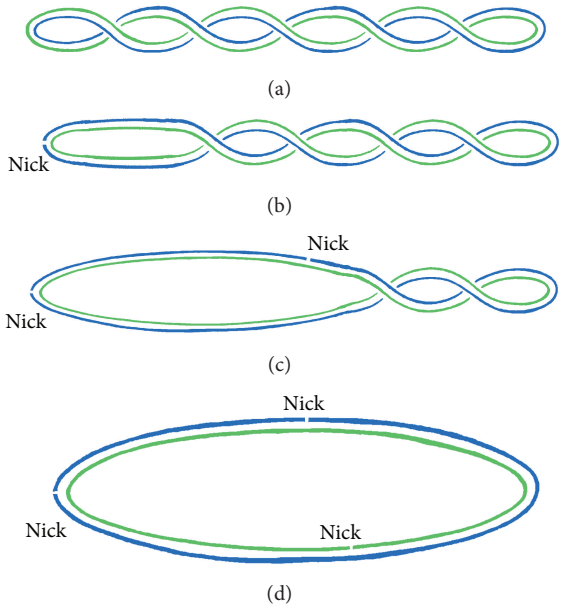

Figure 6: Schematic of the configuration transition of the free circular DNA system under the influence of nicks. (a) Torsional energy of natural DNA with negative supercoil cannot be released and leads to configuration of intersecting state; (b) torsional energy of circular DNA can be partially released by a nick and the intersecting form of some DNA segments changes to the flat circular form; (c) torsional energy of free DNA system is progressively released by nicks; (d) torsional energy of free DNA system is completely released by nicks, and the intersecting form changes to the flat circular form.

influence of nicks. Here, we provide the method to measure configurations by means of AFM observation. Further, based on the quantitative results of configuration transitions, the transmission length of torsional energy in the free DNA system is studied in detail.

The configuration transitions of circular DNA induced by nicks can be explained as follows. In the absence of nicks, natural circular DNA exhibits negative supercoiling [20] (Figure 6(a)). In our experiment, this torsional energy accounts for the occurrence of intersecting state in 25% of the total configurations. According to the nicking angle of pUC19 DNA topological map, two nicks are near the position of a pUC19 DNA molecule that can be viewed as one nick. Based on the calculated results of effective length, one nick only partially releases a torsional energy of 233 bp in the free circular DNA system, thereby resulting in the simplification of complicated configurations with the intersecting state (Figure 6(b)). However, local segments of circular DNA molecules still exhibit the intersecting form because of the transmission limitation of torsional energy. As the number of nicks increases, a greater amount of torsional energy in circular DNA is also released, leading to further simplification of the complicated configuration with intersecting state (Figure 6(c)). Finally, the number of nicks is large enough to release the torsional energy of natural DNA completely (Figure 6(d)).

4. Conclusions

In summary, we developed a new method to study quantitatively the configuration transitions of free circular DNA system with different numbers of nicks using AFM. Free circular DNA has two configuration states. Configuration transitions between intersecting and flat circular states occur in the presence of different numbers of nicks. We defined the nicking angle of DNA topological map and the effective length of torsional energy and found that a torsional energy of 233 bp can be completely released by a nick. Furthermore, based on experimental and quantitative results, we propose a mechanism that explains the configuration transition of the free circular DNA system induced by nicks. In the free DNA system, nicks can release torsional energy so that the complicated configuration of intersecting state becomes simplified. These results and the presented method are important for elucidating the physical mechanism of nicks in the free DNA system.

Conflict of Interests

The authors declare that there is no conflict of interests regarding the publication of this paper.

Acknowledgments

This research was supported by the National Natural Science Foundation of China (Grant 11274374) and the Natural Science Foundation of Shandong Province of China (Grant ZR2014AQ025).

References

[1] T. Lindahl, "Instability and decay of the primary structure of DNA," *Nature*, vol. 362, no. 6422, pp. 709–715, 1993.

[2] S. Shuman and J. Turner, "Site-specific interaction of vaccinia virus topoisomerase I with base and sugar moieties in duplex DNA," *The Journal of Biological Chemistry*, vol. 268, no. 25, pp. 18943–18950, 1993.

[3] S. N. Huang, S. Ghosh, and Y. Pommier, "Topoisomerase I alone is sufficient to produce short DNA deletions and can also reverse nicks at ribonucleotide sites," *Journal of Biological Chemistry*, vol. 290, no. 22, pp. 14068–14076, 2015.

[4] E. Seeberg, L. Eide, and M. Bjørås, "The base excision repair pathway," *Trends in Biochemical Sciences*, vol. 20, no. 10, pp. 391–397, 1995.

[5] H. Wang and J. B. Hays, "Simple and rapid preparation of gapped plasmid DNA for incorporation of oligomers containing specific DNA lesions," *Molecular Biotechnology*, vol. 19, no. 2, pp. 133–140, 2001.

[6] L. Davis and N. Maizels, "Homology-directed repair of DNA nicks via pathways distinct from canonical double-strand break repair," *Proceedings of the National Academy of Sciences of the United States of America*, vol. 111, no. 10, pp. E924–E932, 2014.

[7] H. Wang and J. B. Hays, "Mismatch repair in human nuclear extracts. Quantitative analyses of excision of nicked circular mismatched DNA substrates, constructed by a new technique employing synthetic oligonucleotides," *Journal of Biological Chemistry*, vol. 277, no. 29, pp. 26136–26142, 2002.

[8] F. A. Ran, P. D. Hsu, C. Y. Lin et al., "Double nicking by RNA-guided CRISPR Cas9 for enhanced genome editing specificity," *Cell*, vol. 154, pp. 1380–1389, 2013.

[9] L. Y. Xue, X. M. Zhou, and D. Xing, "Sensitive and homogeneous protein detection based on target-triggered aptamer hairpin switch and nicking enzyme assisted fluorescence signal amplification," *Analytical Chemistry*, vol. 84, no. 8, pp. 3507–3513, 2012.

[10] F. Gao, J. Lei, and H. Ju, "Assistant DNA recycling with nicking endonuclease and molecular beacon for signal amplification using a target-complementary arched structure," *Chemical Communications*, vol. 49, no. 38, pp. 4006–4008, 2013.

[11] M. R. Sawaya, R. Prasad, S. H. Wilson, J. Kraut, and H. Pelletier, "Crystal structures of human DNA polymerase β complexed with gapped and nicked DNA: evidence for an induced fit mechanism," *Biochemistry*, vol. 36, no. 37, pp. 11205–11215, 1997.

[12] W. H. Han, S. M. Lindsay, M. Dlakic, and R. E. Harrington, "Kinked DNA," *Nature*, vol. 386, no. 6625, p. 563, 1997.

[13] S.-H. Chan, B. L. Stoddard, and S.-Y. Xu, "Natural and engineered nicking endonucleases—from cleavage mechanism to engineering of strand-specificity," *Nucleic Acids Research*, vol. 39, no. 1, pp. 1–18, 2011.

[14] B.-C. Yin, Y.-Q. Liu, and B.-C. Ye, "Sensitive detection of microRNA in complex biological samples via enzymatic signal amplification using DNA polymerase coupled with nicking endonuclease," *Analytical Chemistry*, vol. 85, no. 23, pp. 11487–11493, 2013.

[15] R.-Y. Wang, Z.-Y. Shi, Y.-Y. Guo, J.-C. Chen, and G.-Q. Chen, "DNA fragments assembly based on nicking enzyme system," *PLoS ONE*, vol. 8, no. 3, Article ID e57943, 2013.

[16] C. Ji, L.-Y. Zhang, X.-M. Hou, S.-X. Dou, and P.-Y. Wang, "Effect of cisplatin on the flexibility of linear DNA," *Chinese Physics Letters*, vol. 28, no. 6, Article ID 068702, 2011.

[17] X.-M. Hou, X.-H. Zhang, K.-J. Wei et al., "Cisplatin induces loop structures and condensation of single DNA molecules," *Nucleic Acids Research*, vol. 37, no. 5, pp. 1400–1410, 2009.

[18] G. Zuccheri, R. T. Dame, M. Aquila, M. I. Muzzalupo, and B. Samorì, "Conformational fluctuations of supercoiled DNA molecules observed in real time with a scanning force microscope," *Applied Physics A: Materials Science & Processing*, vol. 66, supplement 1, pp. S585–S589, 1998.

[19] W.-J. Chung, Y. Cui, and I. C. Hsu, "The effect of tension on closely spaced nicks in naked DNA molecules," *Biophysical Journal*, vol. 102, no. 3, p. 579a, 2012.

[20] D. E. Pulleyblank, M. Shure, D. Tang, J. Vinograd, and H. P. Vosberg, "Action of nicking-closing enzyme on supercoiled and nonsupercoiled closed circular DNA: formation of a Boltzmann distribution of topological isomers," *Proceedings of the National Academy of Sciences of the United States of America*, vol. 72, no. 11, pp. 4280–4284, 1975.